

Effect of ausforming deformation on creep strength of G91 steel

J.Vivas¹, C.Capdevila^{1*}, M. Serrano², E. Altstadt³ and D. San Martín¹

¹ Centro Nacional de Investigaciones Metalúrgicas (CENIM-CSIC), Avda Gregorio del Amo, 8; Madrid, E-28040, Spain

² División de Materiales Estructurales, Centro Investigaciones Medioambientales y tecnológicas (CIEMAT), Avda. Complutense 22, 28040 Madrid, Spain

³ Helmholtz-Zentrum Dresden-Rossendorf, Bautzner Landstraße 400, 01328 Dresden, Germany

Abstract: Ausforming thermomechanical treatment has been considered as a potential processing route to improve creep strength of 9Cr ferritic/martensitic steels beyond 600 °C. The concept behind this route is to boost the high temperature strengthening mechanisms that come mainly from the combination of solid solution effect and precipitation hardening by thermally stable MX nanoprecipitates generated during subsequent tempering. The ausforming thermomechanical treatment is divided in three steps, austenitization, deformation and tempering. The objective of this work is to discuss the effect of ausforming deformation on austenite in the resultant martensitic microstructure paying special attention to the size, number density and distribution of MX carbonitrides formed after tempering. The microstructural results suggest that the ausforming promote an increase in the number density of MX nanoprecipitates up to 3 order of magnitude as compare to conventional processing route for 9Cr ferritic-martensitic steels. However, an ausforming temperature too high induces the dynamic recrystallisation of austenite mitigating the effects that strained austenite has on subsequent tempered martensite. The creep strength at 700 °C was evaluated by small punch creep tests. The creep results after ausforming were compared to those obtained after conventional heat treatment concluding, in general, that ausforming boosts the creep strength of the steel at 700 °C.

1. INTRODUCTION

The 9Cr ferritic/martensitic steels have been widely used for nuclear applications due to their high swelling resistant. The disadvantage of these steels is their loss of strength beyond 600 °C, so they need to be optimized to guarantee their use in the future nuclear power plants [1]. One of the most promising ideas is applying a thermomechanical treatment (TMT) instead of a conventional treatment. The main contribution of the TMT is the ausforming, which, as other authors have reported, allows increasing considerably the number density of the thermally stable precipitates, i.e MX nanoprecipitates. Consequently, the creep strength is improved greatly [2-6].

In order to develop the best creep resistant microstructure and to optimize the TMT, two grades of deformation 20% and 40% at 900°C are studied in this work. The effect that ausforming deformation has on the morphology of the resultant martensite and their precipitation distribution are evaluated. Finally, a quick screening of creep strength by means of small punch creep (SPC) tests is presented.

2. MATERIALS AND METHODS

A commercial G91 ferritic/martensitic steel in the form of a plate was used to apply the Thermomechanical Treatment. The nominal chemical composition of the steel is shown in Table 1. The conventional processing (CT) of this steel consists on normalization at 1040 °C for 30 minutes followed by tempering at 730 °C for 1 h, and finally air cooling to room temperature.

Table 1. Chemical composition of G91 steel

Elements	C	Si	Mn	Cr	Mo	V	Nb	N	Fe
Wt. %.	0.1	0.4	0.4	9	1	0.2	0.07	0.038	balance

* ccm@cenim.csic.es / Phone: +34 5538900

The TMT was simulated in a Bähr DIL 805A/D plastodilatometer. Cylindrical samples with 10 mm length x 5 mm diameter were deformed at 0.1 s^{-1} . Samples were heated at $5 \text{ }^\circ\text{C/s}$ and cooled at $50 \text{ }^\circ\text{C/s}$. After ausforming procedure XRD studies were carried out with Co-K α radiation in a Bruker AXS D8 diffractometer equipped with Goebel mirror optics and a LynxEye Linear Position Sensitive Detector for ultra-fast XRD measurements in order to obtain dislocations density.

The M_{23}C_6 precipitates were disclosed using a solution of 5 ml hydrochloric acid, 1 g of picric acid and 100 ml of ethyl alcohol (Vilella's reagent). The observation of these precipitates was carried out in a JEOL JSM 6500 FEG-SEM. EBSD measurements mapping with a step size of $0.4 \text{ }\mu\text{m}$ were performed to study the morphology of the martensite. CHANNEL 5 software of Oxford Instruments has been used to process the IPF maps obtained.

The observation of the MX nanoprecipitates was performed in a JEOL JEM 3000F. For this goal, disks of 3 mm in diameter and $80 \text{ }\mu\text{m}$ in thickness were prepared. Then, twin-jet electropolishing was performed at $25 \text{ }^\circ\text{C}$ and 40 V using an electrolyte compose of 95 % acetic acid and 5 % percloric acid. The set up of small punch creep (SPC) tests is presented in Fig. 1, and consists in a lower and upper die connected via a thread to ensure the clamping of cylindrical sample with a thickness of $500 \text{ }\mu\text{m}$ and a diameter of 8 mm. The load is applied by a ceramic punch ball of 2.5 mm in diameter which is in contact with the sample. A plunger rod is used to transmit the dead weight load to the punch ball. All these components are made of Al_2O_3 ceramics. An electrical heater and a thermal insulation surround the clamping device.

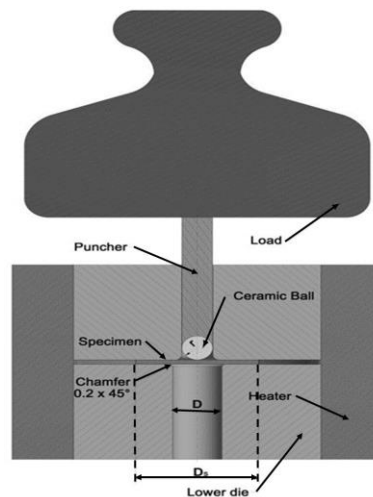


Figure 1. Experimental set-up for small punch creep (SPC) tests

3. RESULTS AND DISCUSSION

2.1. Thermomechanical treatment description

The TMT proposed in this work is divided in different parts. The first one is the austenitisation stage. The target here is to promote almost full solid solution in austenite of alloying elements. This fact will allow maximizing the amount of precipitates available during tempering stage after ausforming. According to thermodynamic calculation made with ThermoCalc® the temperature where this objective is reached is $1225 \text{ }^\circ\text{C}$. This austenitization temperature was hold during 5 minutes to guarantee the homogenization of the sample. The temperature calculated takes into account the suppression of δ -ferrite. The second part is the ausforming itself. The ausforming temperature selected was $900 \text{ }^\circ\text{C}$ following the conventional hot-rolling practice of 9Cr ferritic-martensitic steels. In this stage, compression ratios of 20% and 40% are applied on austenite to generate a highly dislocated austenitic microstructure. These dislocations introduced during ausforming will refine the martensitic microstructure, and will promote a highly dislocated martensite with increasing number of potential nucleation sites for precipitation during subsequent tempering after ausforming.

The last part of the TMT is the tempering. The tempering parameters chosen in this TMT are very similar to those in a conventional tempering stage for 9Cr ferritic-martensitic steel, and its objective is to achieve the optimal precipitate distribution. The tempering parameter selected are $740 \text{ }^\circ\text{C}$ during 45 minutes.

2.2. Effect of ausforming on martensitic microstructure after tempering

Dislocations density in the fresh martensite obtained after ausforming was determined by XRD in order to quantify the effect of the different deformation levels studied. The dislocations density obtained were 1.90×10^{15} and 2.24×10^{15} (m^{-2}) for the deformation ratios of 20% and 40%, respectively. These values are very similar, which might lead us to think that the increase in deformation ratio in ausforming does not increase the dislocations density. This result, in principle, seems contradictory to the philosophy of ausforming treatment, but could be explained in basis of the high deformation temperature chosen for ausforming procedure, i.e. 900 °C. This temperature is sufficiently high to produce annihilation of dislocations during ausforming, limiting therefore the dislocation number that can be inherited after the martensitic transformation. Figures 2(a) and 2(b) show IPF map after tempering for the two samples studied. A very similar martensitic microstructure is observed in terms of block size. This result is in agreement with the dislocations density measured on the previous fresh martensitic microstructure. The deformed austenite prior to martensitic transformation possess similar dislocations density, and in consequence, the resultant martensitic microstructures present the same morphology.

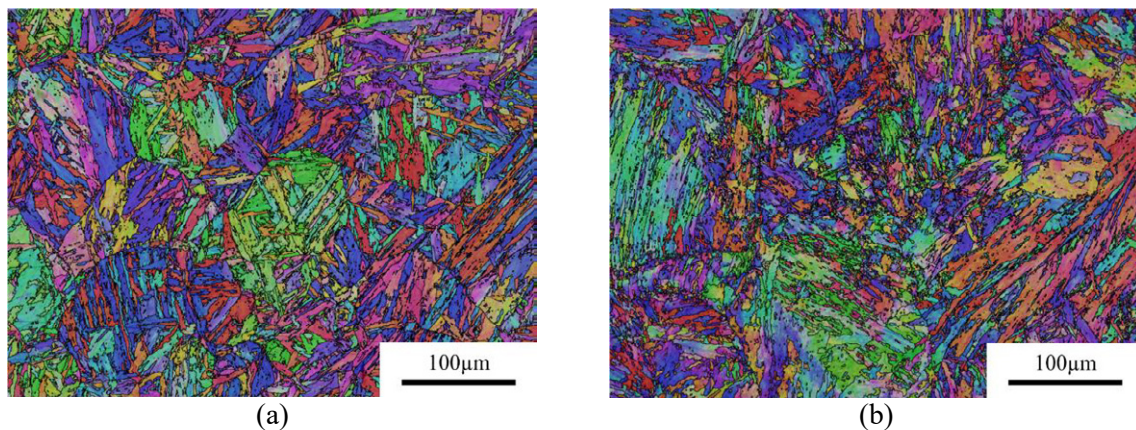


Figure 2. IPF map for the (a) 20%-ausformed tempered martensite, and (b) 40%-ausformed tempered martensite

2.3. Effect of ausforming on precipitates distribution after tempering

Figure 3(a) and 3(b) show SEM micrographs illustrating the M_{23}C_6 precipitates distribution after tempering for both ausformed conditions. Size and number density of M_{23}C_6 carbides is very similar after both ausforming deformation. The number density of these carbides was calculated to be in the order of 10^{19} m^{-3} . This value is in the same order of magnitude that the one reported by Klueh et al. [7] after conventional heat treatments.

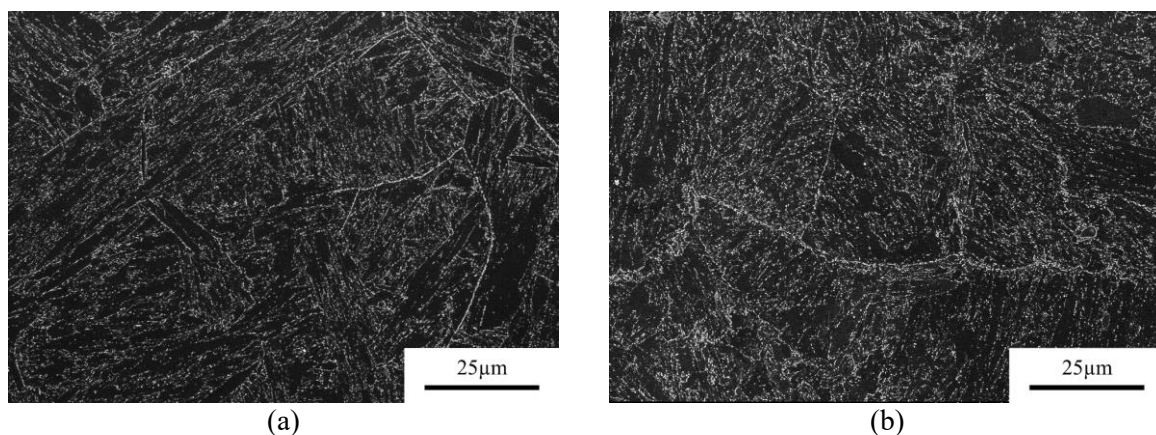


Figure 3. SEM micrographs showing M_{23}C_6 precipitates distribution for (a) 20%-ausformed tempered martensite, and (b) 40%-ausformed tempered martensite

Figures 4(a) and 4(b) show TEM micrographs illustrating the distribution of MX nanoprecipitates after tempering for both ausformed deformation ratios. The size of these nanoprecipitates is ranging from 5 to 10 nm for both ausforming conditions. Such nanometric in size MX carbo-nitrides are even

smaller than those reported in bibliography after conventional heat treatment, which present an average value of 32 nm in diameter [7]. Regarding the number density, both ausforming conditions under study exhibited a number density in the order of 10^{22} m^{-3} . This value is 4 order of magnitude higher than the one obtained for this ferritic-martensitic steel after conventional heat treatment, i.e. 10^{18} m^{-3} as reported in Ref. [7].

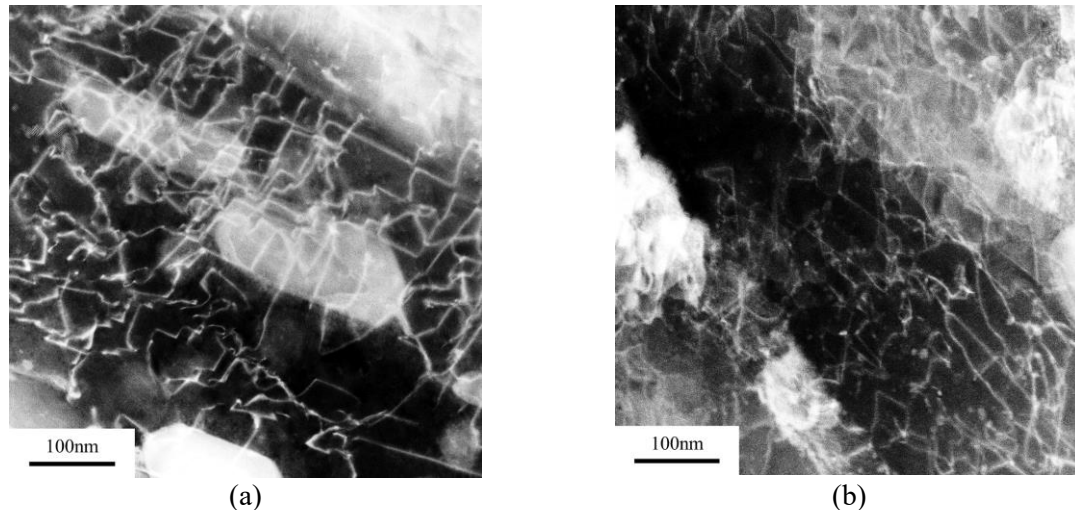


Figure 4. TEM micrographs showing MX nanoprecipitate distribution for (a) 20%-ausformed tempered martensite, and (b) 40%-ausformed tempered martensite

An example of SPCT curves at 200 N exhibiting the variation of specimen deflection with time is shown in Fig. 5 for the ausformed samples at 20% and 40% deformation, and the conventionally process (CT). The curve exhibits the three stages of creep similar to that obtained from a uniaxial creep tests. First, after the instantaneous deflection, bending is the main deformation mode in primary stage. In the secondary and tertiary stage stretching is the prominent deformation mode.

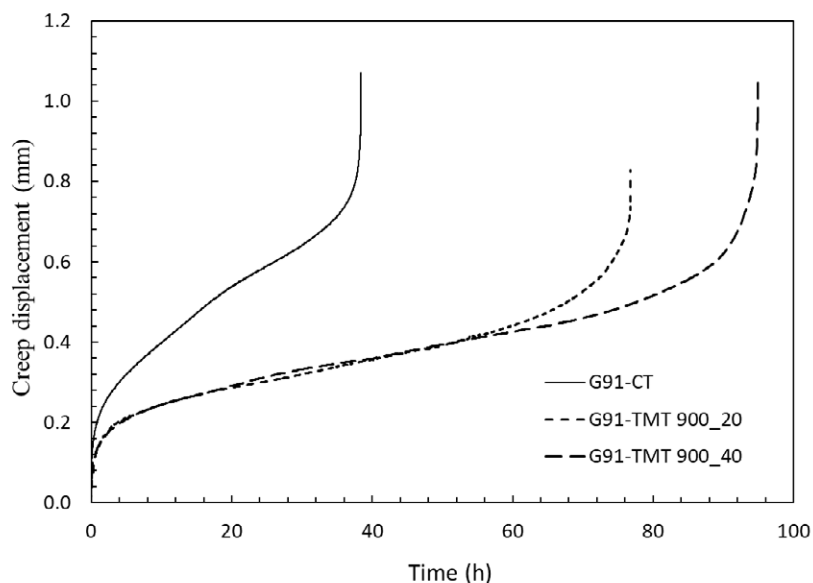


Figure 5. SPC test curves for all material tested at 700 °C with a load of 200N.

3. CONCLUSIONS

The results obtained in this work allow the authors to conclude that:

1. The morphology and block size of the ausformed tempered martensite depends on the dislocations density introduced during ausforming. Dynamic recrystallization during ausforming decreases the dislocations density introduced in austenite and diminish the effect of the ausforming on the martensitic

microstructure.

2. Similar size and number density of MX nanoprecipitates and $M_{23}C_6$ precipitates was obtained for both ausformed tempered martensites. This is consistent with the same dislocation density measured on fresh martensite for both ausforming conditions, since equivalent number of potential nucleation sites for precipitation during tempering is expected.

3. The ausforming increases in four order of magnitude the number density of MX nanoprecipitates in comparison to this steel processed by conventional heat treatment. This fact induce a significant lower minimum creep rate at 700 °C as determined by SPC tests.

Acknowledgements: Authors acknowledge financial support to Spanish Ministerio de Economía y Competitividad (MINECO) in the form of a Coordinate Project (MAT2016-80875-C3-1-R). The work presented here is done within the Joint Programme on Nuclear Materials of the European Energy Research Alliance Pilot Project CREMAR. Authors also would like to acknowledge financial support to Comunidad de Madrid through DIMMAT-CM_S2013/MIT-2775 project. The authors are grateful to Mr. Javier Vara, Mr. Alberto Delgado and Mr. Alberto López for the experimental support. J. Vivas acknowledges financial support in the form of a FPI Grant BES-2014-069863.

REFERENCES

- [1]. K.H. Mayer, F. Masuyama, Creep-Resistant Steels, (editors: F. Abe, T.U. Kern and R. Viswanathan), Woodhead Publishing (2008), 15-77.
- [2]. R.L. Klueh, N. Hashimoto, P.J. Maziasz, Scripta Materialia, 53 (2005) 275-280.
- [3]. S. Hollner, B. Fournier, J. Le Pendu, T. Cozzika, I. Tournié, J.C. Brachet, A. Pineau, Journal of Nuclear Materials, 405 (2010) 101-108.
- [4]. L. Tan, J.T. Busby, P.J. Maziasz, Y. Yamamoto, Journal of Nuclear Materials, 441 (2013) 713-717.
- [5]. J. Vivas, C. Celada-Casero, D. San Martín, M. Serrano, E. Urones-Garrote, P. Adeva, M.M. Aranda, C. Capdevila, Metallurgical and Materials Transactions A, (2016) 1-8.
- [6]. J. Vivas, C. Capdevila, J. Jimenez, M. Benito-Alfonso, D. San-Martin, Metals, 7 (2017) 236.
- [7]. R.L. Klueh, N. Hashimoto, P.J. Maziasz, Journal of Nuclear Materials, 367-370, Part A (2007) 48-53.